

ConMamba: Contrastive Vision Mamba for Plant Disease Detection

Abdullah Al Mamun^{a,b,c}, Miaohua Zhang^b, David Ahmedt-Aristizabal^b, Zeeshan Hayder^b, Mohammad Awrangjeb^a

^a*School of Information and Communication Technology, Griffith University, Nathan, 4111, Queensland, Australia.*

^b*Imaging and Computer Vision Group, Data61, CSIRO, Black Mountain, 2601, Canberra, Australia*

^c*Department of Electrical and Electronic Engineering, Feni University, Feni, 3900, Bangladesh*

Abstract

Plant Disease Detection (PDD) is a key aspect of precision agriculture. However, existing deep learning methods often rely on extensively annotated datasets, which are time-consuming and costly to generate. Self-supervised Learning (SSL) offers a promising alternative by exploiting the abundance of unlabeled data. However, most existing SSL approaches suffer from high computational costs due to convolutional neural networks or transformer-based architectures. Additionally, they struggle to capture long-range dependencies in visual representation and rely on static loss functions that fail to align local and global features effectively. To address these challenges, we propose ConMamba, a novel SSL framework specially designed for PDD. ConMamba integrates the Vision Mamba Encoder (VME), which employs a bidirectional State Space Model (SSM) to capture long-range dependencies efficiently. Furthermore, we introduce a dual-level contrastive loss with dynamic weight adjustment to optimize local-global feature alignment. Experimental results on three benchmark datasets demonstrate that ConMamba significantly outperforms state-of-the-art methods across multiple evaluation metrics. This provides an efficient and robust solution for PDD.

Keywords: Self-supervised learning, Plant disease detection, Contrastive learning, Vision Mamba, dual-level contrastive loss, Dynamic weight adjustment.

1. Introduction

Plant diseases pose a significant threat to crop growth and fruit production, leading to reductions in both yield and quality, resulting in major economic losses [1]. Studies indicate that plant diseases contribute to approximately 20%-40% of global crop yield losses [2]. As illustrated in Figure 1, plant leaf diseases manifest in various forms. By



Figure 1: Sample images of affected plant leaves showing visible symptoms of the disease.

closely examining leaf symptoms, accurate detection becomes possible, allowing for timely intervention and effective treatment [3].

Traditionally, plant disease diagnosis relied on human expertise, a time-consuming, labour-intensive process, and prone to errors due to the vast diversity of plant diseases [4]. With the success of deep learning approaches across various domains, including agriculture [5, 6, 7], researchers have increasingly adopted these models to improve the accuracy and efficiency of plant leaf disease detection. Deep learning enables large-scale crop monitoring while reducing the costs associated with manual diagnosis [8]. Nonetheless, challenges persist due to the complexity of plant disease identification and the limited availability of labeled training data.

Deep learning-based approaches for plant disease identification generally fall into three main categories: model enhancement [9], Few-shot Learning (FSL) [10], and Self-Supervised Learning (SSL) [11]. Some studies also explore dataset augmentation using Generative Adversarial Networks (GANs) [12, 13], though this topic falls outside the scope of this discussion. Specifically, model enhancement primarily focuses on improving disease detection models by incorporating advanced architectures, such as Convolutional Neural Networks (CNNs) [14] and transformers [15]. While these approaches achieve high accuracy, they rely on supervised learning, which demands large amounts of labeled data. To address data scarcity, FSL strategies train models to identify similarities between samples and transfer this knowledge to new domains using only a small labeled dataset (support set). However, its effectiveness declines when the source domain differs considerably from the target dataset, limiting its broader applicability.

SSL has emerged as a powerful approach for Plant Disease Detection (PDD) [16], addressing the challenges of limited labeled data by leveraging supervisory signals from raw, unlabeled datasets. Recent advancements in deep learning have significantly improved image-based disease identification, and the integration of SSL further enhances these capabilities by maximizing data utilization and improving model efficiency. By reducing

reliance on annotated datasets, SSL offers a scalable and robust framework for modern PDD systems [17].

SSL techniques can be broadly classified into Contrastive Learning (CL) and Generative Learning (GL) [18]. GL methods aim to reconstruct or predict parts of input data, as seen in works by Kim et al. [19] and Jin et al. [20]. On the other hand, CL has emerged as a dominant approach due to its effectiveness and simplicity for vision-related tasks [21, 22]. CL focuses on distinguishing positive pairs, such as augmented versions of the same image, from negative pairs, which are different images. This method has proven highly successful in capturing meaningful semantic representations, often achieving results comparable to or better than supervised learning on various downstream applications.

Traditional convolutional networks, such as ResNet50 [23], EfficientNetB0 [24], and VGG16 [25], are widely used for feature extraction in CL frameworks. However, they primarily capture local features, limiting their ability to represent global information. The transformer-based frameworks [26, 27] have better abilities to capture global information. However, the quadratic complexity of their inherent self-attention mechanism makes them computationally expensive.

These constraints hinder the efficient detection of complex, distributed disease symptoms in plants. Long-range dependencies are crucial for robust classification, as they enhance resilience to noise, occlusions, and environmental variations [28]. Additionally, static loss functions in CL restrict feature alignment across local and global scales, impacting adaptability and generalization to unseen disease scenarios [29].

Recently, Mamba network [30, 31], which is a new deep learning architecture based on the SSM focuses on sequence modeling and offers several distinct advantages. By leveraging a state-space formulation, it efficiently captures long-range dependencies with linear computational complexity, which makes it more efficient than traditional self-attention mechanisms. This efficiency is especially beneficial when processing high-resolution plant disease images. Mamba’s superior performance in capturing long-range dependencies is particularly important for PDD because disease symptoms can appear as subtle, scattered patterns across a leaf. By enhancing these long-range correlations, the model can integrate information from various regions of the leaves/plants, thus producing more accurate disease predictions. For detailed information on Vision Mamba and its significance in PDD, readers are referred to Sections 4.1 and 4.2, respectively.

Considering the advantages of the Mamba-network, we propose a Contrastive Mamba network (ConMamba) to address the above-mentioned challenges for PDD. Specifically, a contrastive self-supervised learning framework based on Mamba is proposed by leveraging the Vision Mamba Encoder (VME) along with dual-view patch embedding techniques. This design enables the extraction of robust and rich visual representation by capturing both fine-grained local features as well as global context. Besides, the proposed framework incorporates dynamic feature alignment across both local and global scales, effectively capturing intricate spatial patterns and long-range dependencies. This enhanced feature integration is important to achieving robust and accurate PDD in complex real-world scenarios

The key contributions of this work include:

- A self-supervised Contrastive Vision Mamba (ConMamba) framework is developed specially tailored for plant disease detection. ConMamba integrates a bidirectional State Space Model (SSM) to efficiently capture long-range contextual relationships, enabling robust visual representation of subtle, localized symptoms and complex global disease patterns.
- A dual-level contrastive learning strategy consisting of intra/inter-class contrastive learning is developed to both promote local embedding consistency across augmented image views and enforce global discriminability between embeddings of distinct disease classes. The dual approach ensures comprehensive representation learning, addressing the critical need for effective local-global feature alignment.
- To adaptively balance the intra- and inter-contrastive losses during training, a dynamic weighting mechanism based on learnable uncertainty parameters is designed. This mechanism significantly enhances training robustness and generalization performance, resulting in highly discriminative embeddings suitable for accurate disease classification.

The remainder of the paper is organized as follows: Section 2 presents a literature review and motivation on PDD using self-supervised CL. Section 3 explains the preliminaries of VM, including its advantages on plant diseases. Section 4 details the proposed ConMamba framework. Section 5 evaluates ConMamba on three benchmark datasets:

PlantVillage, PlantDoc, and Citrus. Finally, Section 6 concludes the work and discusses directions for future work.

2. Related Works and Motivations

2.1. Related Works

Li et al. [32] initially focused on enhancing image analysis and classification for PDD using publicly labeled datasets in a supervised learning setting. In contrast, Fang et al. [33] introduced a self-supervised Cross-Iterative Kernel-Based Image Clustering System (CIKICS) for PDD, leveraging cross-iterative Kernel K-means to produce pseudo-labeled training sets. While effective, its offline computations and slow processing speed hindered scalability on large datasets. Yang et al. [34] proposed a self-supervised mechanism for tomato disease detection, using a feedback model to optimize fine-grained categorization based on three localized regions of tomato leaf samples. Despite achieving high accuracy, the method was limited to tomato diseases, required balanced class distributions, and introduced significant computational overhead due to the use of multiple models.

Beyond domain-specific applications, general SSL frameworks have contributed to visual representation learning. BYOL [35] eliminated the need for negative pairs in CL by employing an online target network setup, where the target network was updated through a slow-moving average of the online network’s weights. While achieving state-of-the-art results on ImageNet and transfer tasks, BYOL relied heavily on augmentations, lacked theoretical guarantees to prevent collapse, and incurred high computational costs. SimSiam [36] further simplified SSL by introducing a Siamese network that removed negative pairs, momentum encoders, and large batch requirements. It prevented representation collapse through a stop-gradient operation, achieving competitive performance on ImageNet. However, its strong dependence on data augmentations and the absence of theoretical justification for the stop-gradient mechanism remain notable limitations.

CIKICS [33] advanced self-supervised clustering by combining Kernel K-means with deep learning techniques to group unlabeled plant disease images. It generated refined clusters using a CNN classifier, a ResNet50-based similarity finder, and a Siamese network. While effective on both balanced and unbalanced datasets, its iterative nature and high computational cost limited real-time applicability.

Zhang et al. [37] utilized SimCLR for cassava leaf disease detection, achieving high

accuracy but depending heavily on large batch sizes and data augmentation, which limited its effectiveness on diverse datasets. Similarly, Bunyang et al. [24] applied SimCLR as a pre-trained model for plant disease classification but required substantial memory and computational resources.

Several studies have explored ViTs for PDD. Zhang et al. [38] employed entropy masking for tea disease classification, but this approach risked losing critical information during sampling. Yu et al. [39] proposed a mixed-attention ViT for ultra-fine categorization. However, its high parameter count posed challenges in accurately predicting disease regions. Meng et al. [40] used a pre-trained ViT to classify known and unknown plant diseases but faced computational complexity and performance degradation when distinguishing between visually similar diseases, emphasizing the need for larger datasets.

Monowar et al. [23] proposed a self-supervised image clustering method for PDD, introducing strategies to improve stability. However, its reliance on random selection and data augmentation reduced generalizability. Similarly, Fang et al. [33] incorporated pre- and post-processing into the CIKICS framework, increasing computational costs and limiting its applicability to offline settings. Zhao et al. [17] introduced CL for Leaf Disease Identification (CLA), leveraging domain adaptation and pre-training to improve generalization on limited labeled and noisy data. However, accuracy varied depending on the mix ratio in the source domain, data size, and class distribution.

2.2. Motivation

The above-mentioned traditional convolutional networks or transformer-based frameworks are either suffering from capturing global and long-range dependencies or huge computational complexity. Besides, these methods employ static loss functions that maximize similarity without aligning local and global features. Recently, Mamba frameworks have been widely applied to capture long-range dependencies in an image and have yielded promising results. However, traditional Mamba architectures are typically designed for supervised learning and depend on large, well-labeled datasets. This makes them less effective in environments where labeled data is scarce, such as in plant disease datasets. Without mechanisms for data imbalance problems, standard Mamba-based models might overfit the majority classes. This can lead to inadequate feature representations for under-represented diseases, limiting the overall detection performance. Existing architectures may struggle to capture the invariant features necessary for robust PDD. Variations in

lighting, angle, and plant condition require the model to learn features that are consistent across these changes, which is a gap that CL is well-suited to address.

Thus, to address these limitations, we propose the Contrastive Mamba (ConMamba) framework for PDD. It has the following advantages: it can harness large amounts of unlabeled data by learning invariant features from different augmentations of the same image. This is particularly useful in PDD, where obtaining labeled data is challenging. By training the model to distinguish between different augmented views of the same plant image (positive pairs) and different plant images (negative pairs), CL forces the model to focus on essential, disease-relevant features. CL can also help to balance the representation learning process by emphasizing the similarity between different views of the same disease condition, rather than relying solely on class labels that might be skewed. All these benefits will contribute to learning more discriminative and robust feature representations, which can improve PDD accuracy.

3. Preliminaries

3.1. State Space Model (SSM)

SSMs mathematically describe continuous linear systems using structured linear differential equations. An SSM transforms an input sequence $x(t) \in \mathbb{R}^L$ into an output sequence $y(t) \in \mathbb{R}^L$ through an intermediate hidden state $h(t) \in \mathbb{R}^N$. This hidden state evolves according to the state transition matrix $A \in \mathbb{R}^{N \times N}$, influenced by input and output projection parameters $B \in \mathbb{R}^{N \times 1}$ and $C \in \mathbb{R}^{1 \times N}$:

$$h'(t) = Ah(t) + Bx(t), \quad y(t) = Ch(t) + Dx(t). \quad (1)$$

For discrete inputs, which are common in deep learning, discrete parameters \bar{A} and \bar{B} are defined using a time step Δ :

$$\bar{A} = \exp(\Delta A), \quad \bar{B} = (\Delta A)^{-1}(\exp(\Delta A) - I)\Delta B, \quad (2)$$

resulting in a discrete model:

$$h_t = \bar{A}h_{t-1} + \bar{B}x_t, \quad y_t = Ch_t. \quad (3)$$

The S4 model [31] uses fixed parameters A , B , C , and Δ across all time steps, enhancing computational efficiency through global convolution but potentially limiting adaptability to specific inputs.

3.2. Selective State Space Model

The selective SSM [30] introduces a time-variant mechanism by dynamically computing the parameters B , C , and Δ based on the input sequence via linear projection, while keeping A fixed. This dynamic adaptation enhances sequence modeling but eliminates the feasibility of global convolution, requiring recurrent processing instead. Although effective for sequential data, this approach limits GPU parallelization, leading to slower performance. To mitigate this issue, the Mamba model integrates a hardware-optimized algorithm that enables efficient GPU utilization for recurrent computations. Designed specifically for one-dimensional sequential data, such as text and audio, Mamba provides a practical solution for tasks requiring adaptive sequence processing.

3.3. Self-supervised Learning with Contrastive Learning

CL is a prominent self-supervised representation learning paradigm, designed to differentiate between similar (positive) and dissimilar (negative) samples within a dataset, enabling the model to learn useful representations without requiring explicit labels [22]. By strategically constructing pairs of data points, this technique brings similar instances closer while pushing dissimilar instances apart in the feature space, facilitating the capture of underlying semantic structures inherent to the data. This process relies heavily on the careful selection of positive and negative samples and the implementation of data augmentation strategies to generate informative contrasts [21]. Notably, CL frameworks such as SimCLR [21], MoCo [41], and BYOL [35] have demonstrated remarkable success across various domains, including computer vision, natural language processing, and speech recognition, achieving performance comparable to supervised learning approaches.

4. Method

In this section, we introduce our proposed contrastive VM framework in details. First, we will give a detailed explanation of the advantages of VM for plant disease detection, and then introduce the contrastive VM step by step.

4.1. Vision Mamba: Rethinking Local-Global Context Modeling

Current deep learning approaches, such as CNNs and Vision Transformers (ViTs), face challenges in capturing both local detailed information and global long-range dependencies

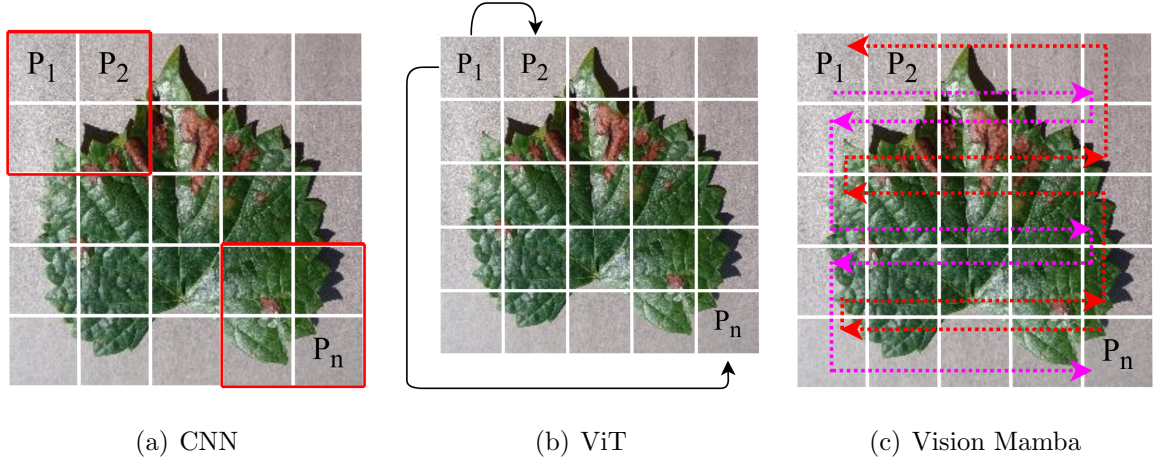


Figure 2: Comparison of different architecture designs: (a) CNN, (b) ViT, and (c) Vision Mamba, emphasizing their capacities to capture short-range and long-range dependencies.

effectively. CNNs utilize an inductive bias that emphasizes local connectivity, processing adjacent regions within an image using predefined kernel sizes, which is defined as:

$$f(x) = \sigma(W * x + b), \quad (4)$$

where $*$ denotes convolution, W is the kernel, and $\sigma(\cdot)$ is a nonlinear activation. This operation effectively captures localized spatial fine detailed patterns, such as spatial relationships between nearby structures, as illustrated by regions P_1 and P_2 in Figure 2 (a). However, CNNs struggle to integrate distant visual features due to their constrained receptive fields, limiting their ability to relate distant areas within an image, such as segment P_1 with P_n . In contrast, ViTs eliminate these fixed inductive biases and treat all image patches equally. They capture global information through self-attention mechanisms and positional encoding to learn spatial relationships across an entire image, which is shown in Figure 2 (b). The self-attention is defined as:

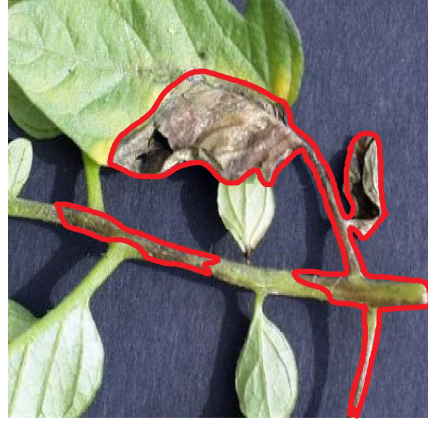
$$\text{Attention}(Q, K, V) = \text{softmax}\left(\frac{QK^T}{\sqrt{d_k}}\right)V, \quad (5)$$

where Q, K, V represent query, key, and value embeddings respectively, and d_k is the embedding dimension. This design enables ViTs to capture global dependencies effectively, making it possible to establish direct connections between widely separated image regions. However, due to this self-attention mechanism, ViTs require extensive data and computational resources to adequately learn local and global features.

To overcome these limitations, the VM introduces a bidirectional SSM [30] to integrate local and global contextual information efficiently. Unlike CNN and ViT, VM models



(a) Affected in a specific region



(b) Affected across different areas

Figure 3: Sample images of plant diseases: (a) affected in a specific region, and (b) affected across different areas, emphasizing the importance of local features and global, long-range dependencies for comprehensive plant disease detection.

visual sequences of image patches bidirectionally, combining localized inductive biases with global dependency modeling. Therefore, the vision mamba is able to learn local dependencies, allowing it to model relationships between adjacent segments (e.g., P_1 and P_2). At the same time, its efficient long-sequence modeling capabilities extend its receptive field across distant regions.

This balanced combination of local and long-range feature extraction makes VM particularly well-suited for PDD, where both local and global information are crucial for accurate disease detection. Figure 2 (c) illustrates how VM’s sequential processing allows it to capture short- and long-range dependencies more effectively than CNNs and ViTs alone.

4.2. Vision Mamba for Robust Plant Diseases

Effective PDD demands the capability to identify subtle localized symptoms and recognize systemic disease patterns [42] distributed across the entire plant. As shown in Figure 3 (a), the plant leaf is affected in a specific region, where local features play a crucial role in accurate classification. In contrast, Figure 3 (b) illustrates the effect of disease on various parts of the plant, highlighting the importance of global and long-range dependencies for identifying multiple affected regions. Thus, both local features and global, long-range dependencies are essential for comprehensive PDD. Vision Mamba’s bidirectional long-sequence modeling efficiently correlates distant regions within plant images.

Suppose an input plant leaf image X is segmented into patches $\{x_1, x_2, \dots, x_M\}$. VM processes this patch sequence through its bidirectional SSM, represented as:

Forward Direction:

$$h_t^{fwd} = \bar{A}h_{t-1}^{fwd} + \bar{B}x_t, \quad y_t^{fwd} = Ch_t^{fwd} \quad (6)$$

Backward Direction:

$$h_t^{bwd} = \bar{A}h_{t-1}^{bwd} + \bar{B}x_t, \quad y_t^{bwd} = Ch_t^{bwd} \quad (7)$$

The final embedding of each patch x_t integrates bidirectional features as:

$$h_t = \text{Fuse}(y_t^{fwd}, y_t^{bwd}) \quad (8)$$

This fusion of forward and backward contexts allows VM to robustly encode fine-grained localized features and complex global patterns, thereby significantly enhancing disease detection accuracy, even in scenarios with subtle or discattered symptoms.

4.3. Contrastive Vision Mamba (ConMamba)

The proposed Contrastive Vision Mamba (ConMamba) framework is specifically designed to effectively leverage self-supervised learning for robust plant disease detection. ConMamba introduces a dual-level contrastive learning approach that simultaneously optimizes embeddings for both local and global discriminability, uniquely integrated with a dynamic uncertainty-based weighting mechanism.

ComMamba consists of three key components:

- **Contrastive Data Augmentation:** We generate semantically consistent yet visually diverse augmented viewers from each original image, forming the positive and negative pairs necessary for contrastive learning.
- **Bidirectional Feature Representation with Vision Mamba:** Leveraging Vision Mamba’s novel bidirectional SSM, we transform augmented image views into highly discriminative embeddings.
- **Dual-level Contrastive Optimization:** we propose two complementary yet distinct contrastive losses, intra-class contrastive loss and inter-class contrastive loss, to optimize local robustness and enforce clear discriminative boundaries among embeddings from distinct disease classes.

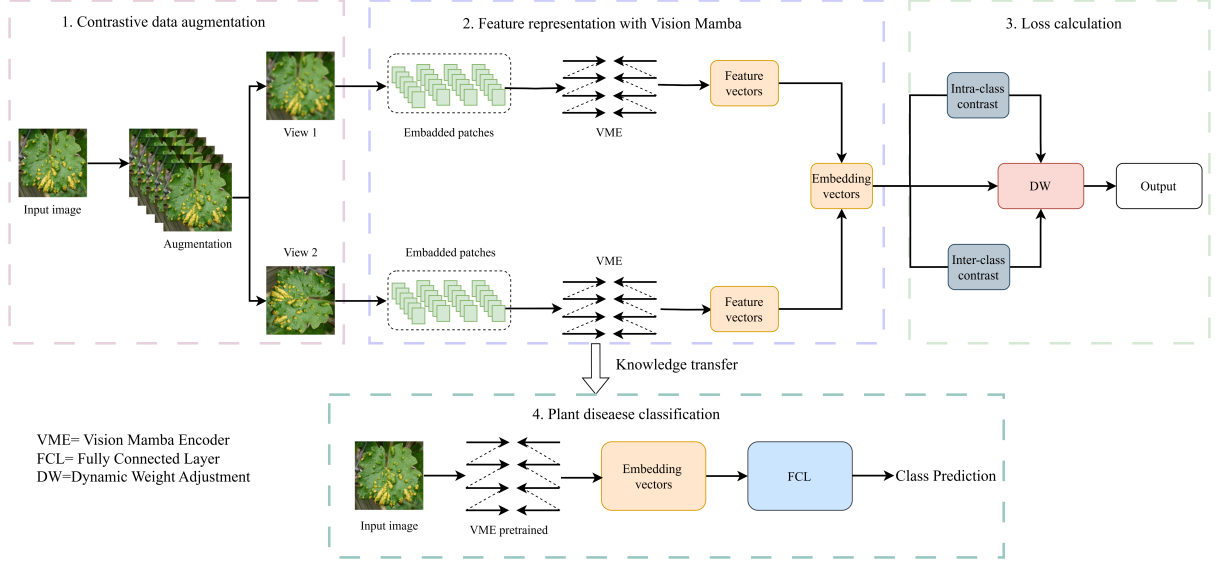


Figure 4: Schematic representation of the ConMamba framework. The framework begins with Stage 1 (Contrastive data augmentation): Data augmentation is applied to input images to generate two distinct augmented views for each input image. Stage 2 (Feature representation with Vision Mamba): Each augmented view undergoes patch embedding followed by the Vision Mamba Encoder (VME) to obtain meaningful bidirectional feature representations. Stage 3 (Loss calculation): A dual-level Contrastive loss with dynamic weight adjustment is employed to maximize local pairwise similarity (intra-class contrast) and global alignment (inter-class contrast). Finally, Stage 4 (Plant disease classification): The plant disease classification task adapts the learned representations for plant disease classification, utilizing the embedding vectors to produce class predictions.

The integration of these three components provides ConMamba with a robust framework to simultaneously capture fine-grained local variations and clear global discriminative structures, significantly enhancing representation quality for plant disease detection tasks. An overview of the proposed model is shown in Figure 4.

4.3.1. Contrastive Data Augmentation

An important step in our Contrastive Mamba framework is the generation of meaningful contrastive samples by data augmentation. Specifically, each original plant disease image X undergoes multiple augmentation operations $T(\cdot)$, resulting in different yet semantically consistent augmented views. Given an original image X , we generate augmented views $X_i = T_i(X)$, where each T_i represents a random transformation, such as rotation, cropping, color jittering, or Gaussian noise addition. The augmented views can be defined as:

$$\mathcal{X} = \{X_1, X_2, \dots, X_n\}, \quad X_i = T_i(X) \quad (9)$$

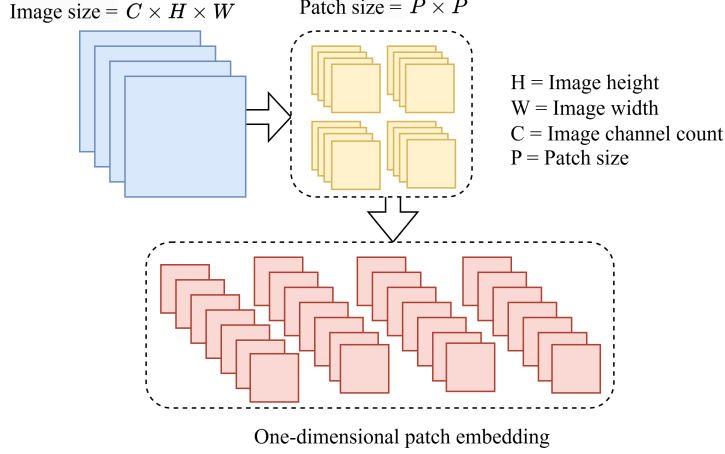


Figure 5: Illustration of the patch embedding process.

These augmented views serve as positive pairs from the same original image for intra-contrastive learning, which will focus on local feature robustness. Simultaneously, augmented views from different original images form negative pairs, utilized inter-contrastive learning to ensure global feature discriminability. This formulation of augmented samples provided the foundational data required for subsequent loss calculation in Section 4.3.3 and facilitates robust, discriminative embedding learning within our Contrastive Vision Mamba framework.

4.3.2. Feature Representation with Mamba

After generating the augmented views as described in Section 4.3.1, we transform each augmented image into discriminative embeddings using the Mamba encoder. Specifically, each augmented image $X_i \in \mathcal{X}_{aug}$ is first divided into a sequence of patches $\{x_i^1, x_i^2, \dots, x_i^M\}$ as shown in Figure 5, where M denotes the total number of patches. Each patch x_i^j is embedded into a lower dimensional representation h_i^j via the Mamba encoder:

$$h_i^j = \text{MambaEncoder}(x_i^j) \quad (10)$$

This step leverages the Mamba’s encoder’s capability to capture rich bidirectional contexts, enabling both local and global features to be robustly represented. These embedded representations $\{h_i^1, h_i^2, \dots, h_i^M\}$ serves as inputs for the subsequent intra- and inter-contrastive loss computations in Section 4.3.3, providing structured, context-rich embeddings that significantly enhance the model’s capability for accurate and robust plant disease detection.

4.3.3. Dual-level Contrastive Learning and Dynamic Weight Adjustment

In our Contrastive Mamba framework, the loss calculation is essential to effectively learning discriminative representations from plant disease images. To achieve a comprehensive embedding space, we propose a dual-level contrastive learning strategy comprising: Intra-Class Contrastive Learning and Inter-Class Contrastive Learning. The intra-class component enhances local feature robustness by maximizing the similarity between embeddings derived from different augmented viewers of the same image, while the inter-class component improves global discriminability by enforcing embeddings from different disease classes to be distinctly separated. Furthermore, we introduce a dynamic weight adjustment mechanism that adaptively combines these two losses to optimize overall performance. An overview of this dual-level contrastive loss with dynamic weight adjustment is shown in Figure 6.

- **Intra-Class Contrast:** Contrastive loss promotes local consistency by ensuring embeddings derived from different augmented views of the same image are closely aligned. It aims to maximize the mutual information (MI) between representations from positive pairs and minimize the MI between representations from negative pairs. Given two augmented views $T_i(X)$ and $T_j(X)$ of an original input X , their embeddings h_i and h_j form a positive pair. Embeddings from different images form negative pairs. Intra-class contrastive learning aims to maximize this mutual information between the augmented views of the same image, thus encouraging embeddings to ignore irrelevant variations (noise, transformations). This optimization corresponds to minimizing the following Normalized Temperature scaled Cross Entropy loss:

$$\mathcal{L}_{intra} = -\frac{1}{N} \sum_{i=1}^N \log \frac{\exp(h_i \cdot h_j / \tau)}{\sum_{k \neq i} \exp(h_i \cdot h_k / \tau)}, \quad (11)$$

where τ represents the temperature parameter controlling the sharpness of similarity distribution, and N is the number of positive pairs in the batch.

The vision mamba framework actually enhances intra-class contrastive learning. Because the vision mamba in this paper uses a Bidirectional State Space Model (SSM), which means it captures both forward and backward context within image patches. By encoding local context from both directions, Mamba gains a richer and more robust local understanding of each image patch, helping to maintain consistent rep-

representations across augmentations. As the intra-class contrastive loss pushes embeddings from augmentations close together, the bidirectional modeling reinforces this robustness because it provides a more stable local representations, less sensitive to irrelevant variations. Embeddings learned via Mamba become robust against subtle, local distortions, leading to improved local feature robustness, allowing the model to identify subtle disease symptoms more reliably in diseased plant images, despite slight variations in image appearance.

- **Inter-Class Contrast:** To ensure global discriminative capability, the inter-class contrastive loss is designed to minimize mutual information between embeddings from different classes, increasing the separability across distinct disease categories. Specifically, this loss enforces a clear embedding space boundary between different disease classes. Embeddings from images of the same class are encouraged to cluster tightly together, while embeddings from distinct classes are pushed apart by at least a margin m . To achieve this, a margin-based contrastive formulation is defined as:

$$\mathcal{L}_{inter} = \frac{1}{N} \sum_{i=1}^N \max(0, m - d(h_i, h_j) + d(h_i, h_k)), \quad (12)$$

where $d(h_i, h_j)$ measures similarity between embeddings of the same class, $d(h_i, h_k)$ measures similarity between embeddings of different classes, and m is a margin ensuring negative pairs remain sufficiently distant. This loss enhances class-level structure, improving the separability of learned features in the embedding space.

As mentioned earlier, we use the mamba framework that leverages a selective bidirectional context via its state-space model, modeling global interactions between patches across the entire image. This long-range dependency modeling means Mamba encodes more global meaningful features, connecting subtle disease indicators across distant image regions. Consequently, Mamba enhances the effectiveness of inter-class contrastive learning because it generates consistent global embeddings, making it easier to separate embeddings of different classes clearly. Global feature separability significantly enhances disease classification performance reducing confusion between classes that may have similar local symptoms but distinct global distributions of patterns. Therefore, these settings leads to embeddings with improved class discriminability, enhancing the accuracy and generalization of the model

across varied disease types.

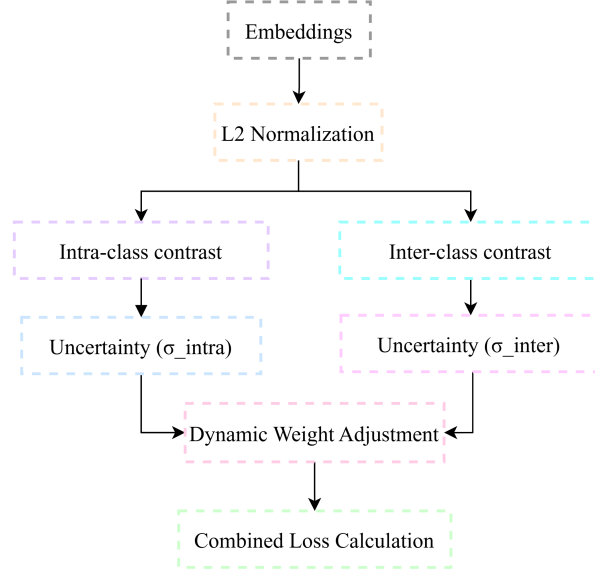


Figure 6: Dual-level Contrastive loss with dynamic weight adjustment.

- **Dynamic Weight Adjustment:** To optimally combine the intra-class contrastive and inter-class contrastive losses, we introduce a dynamic weight adjustment mechanism based on uncertainty modeling. This approach addresses the challenge of effectively balancing the contributions of these two distinct loss functions during the training process. Specifically, we assume that each loss function follows a Gaussian likelihood with uncertainty parameters σ_{intra} and σ_{inter} representing the inherent noise or uncertainty associated with the intra- and inter- class contrastive tasks, respectively.

The likelihood functions can be defined as Gaussian distributions:

$$p(\mathcal{L}_{intra}|\sigma_{intra}) \propto \frac{1}{\sigma_{intra}} \exp\left(-\frac{\mathcal{L}_{intra}}{2\sigma_{intra}^2}\right), p(\mathcal{L}_{inter}|\sigma_{inter}) \propto \frac{1}{\sigma_{inter}} \exp\left(-\frac{\mathcal{L}_{inter}}{2\sigma_{inter}^2}\right), \quad (13)$$

From a Bayesian perspective, maximizing these likelihoods with respect to the uncertainty parameters is equivalent to minimizing the negative log-likelihood(NLL). The NLL for the combined loss can be defined as:

$$-\log p(\mathcal{L}_{intra}, \mathcal{L}_{inter}|\sigma_{intra}, \sigma_{inter}) = -\log[p(\mathcal{L}_{intra}|\sigma_{intra})p(\mathcal{L}_{inter}|\sigma_{inter})] \quad (14)$$

By expanding and simplifying this expression, our dynamic weight adjustment loss

is given by

$$\begin{aligned}\mathcal{L}_{total} &= \frac{1}{2\sigma_{intra}^2}\mathcal{L}_{intra} + \frac{1}{2\sigma_{inter}^2}\mathcal{L}_{inter} + \log(\sigma_{intra} \cdot \sigma_{inter}), \\ \mathcal{L}_{final} &= \frac{1}{N} \sum_{i=1}^N \mathcal{L}_{total}^{(i)},\end{aligned}\tag{15}$$

where the terms $\frac{1}{2\sigma_{intra}^2}$ and $\frac{1}{2\sigma_{inter}^2}$ act as adaptive weight factors, dynamically balancing intra-class contrastive and inter-class contrastive losses based on the learned uncertainty. This ensures that the model places higher weight on the loss with lower uncertainty (higher confidence) and lower weight on the more uncertain loss. The additional term $\log(\sigma_{intra}, \sigma_{inter})$ acts as a regularizer, penalizing the uncertainty terms from becoming excessively large. Without this logarithmic regularization term, the uncertainty parameters could increase indefinitely, minimizing the contribution of both losses and leading to ineffective learning. By introducing this $\log(\cdot)$ term, we encourage the model to find a meaningful trade-off between minimizing individual losses and maintaining manageable uncertainty levels. Based on this analysis, we know that this dynamic uncertainty-based weighting allows the network to adaptively and continuously prioritize either local alignment (intra-class contrastive) or global alignment (inter-class contrastive) based on which aspect requires more attention during training. Therefore, the learned embeddings are highly discriminative, robust, and well-suited for downstream tasks such as PDD classification.

4.4. Plant Disease Classification

The Plant disease classification task, illustrated in Figure 4 (Step 4), processes input images using the pre-trained VME. Trained during the pretext task, the VME extracts meaningful and enriched features, encapsulating them in an embedding vector. This vector serves as a compact yet comprehensive representation of the images, preserving both local and global relationships essential for classification. The embedding vector is then fed into a Fully Connected Layer (FCL), which maps the extracted features to their corresponding output classes. Finally, the FCL produces the predicted class labels, completing the downstream task.

The proposed Contrastive Vision Mamba (ConMamba) for plant disease detection is summarized in Algorithm 1.

Algorithm 1: Contrastive Vision Mamba Framework for Plant Disease Detection

Input: Dataset $\mathcal{D} = \{(X_i, y_i)\}_{i=1}^N$, augmentation $T(\cdot)$, Encoder \mathcal{F}_θ , epochs E , batch size B , margin m , temperature τ , initial uncertainties $\sigma_{intra}, \sigma_{inter}$, learning rate η

Output: Trained encoder parameters \mathcal{F}_{θ^*}

```

1 Initialize parameters  $\theta$  for encoder  $\mathcal{F}_\theta$ ;
2 Initialize uncertainty parameters  $\sigma_{intra}, \sigma_{inter}$ ;
3 for  $epoch = 1, 2, \dots, E$  do
4   for each batch  $\{(X_b, y_b)\}_{b=1}^B$  do
5     // Contrastive Data Augmentation
6     Generate two augmented views per image:  $X_b^1 = T_1(X_b), X_b^2 = T_2(X_b)$ ;
7     // Feature Representation with Mamba
8     Compute embeddings  $h_b^1, h_b^2$  using Mamba encoder:
          
$$h_b^1 = \mathcal{F}_\theta(X_b^1), \quad h_b^2 = \mathcal{F}_\theta(X_b^2)$$

9     // Intra-Class Contrastive Loss (Local Robustness)
          
$$\mathcal{L}_{intra} = -\frac{1}{B} \sum_{b=1}^B \log \frac{\exp(h_b^1 \cdot h_b^2 / \tau)}{\sum_{k \neq b} \exp(h_b^1 \cdot h_k^2 / \tau)}$$

10    // Inter-Class Contrastive Loss (Global Alignment)
11    Select positive embedding  $h_j^1$  from same class, negative embedding  $h_k^1$  from
        different class:
          
$$\mathcal{L}_{inter} = \frac{1}{B} \sum_{b=1}^B \max(0, m - d(h_b^1, h_j^1) + d(h_b^1, h_k^1))$$

12    // Dynamic Weight Adjustment
          
$$\mathcal{L}_{total} = \frac{1}{2\sigma_{intra}^2} \mathcal{L}_{intra} + \frac{1}{2\sigma_{inter}^2} \mathcal{L}_{inter} + \log(\sigma_{intra}\sigma_{inter})$$

13    // Parameter Update
14     $\theta \leftarrow \theta - \eta \nabla_\theta \mathcal{L}_{total}$ 
15     $\sigma_{intra} \leftarrow \sigma_{intra} - \eta \nabla_{\sigma_{intra}} \mathcal{L}_{total}, \quad \sigma_{inter} \leftarrow \sigma_{inter} - \eta \nabla_{\sigma_{inter}} \mathcal{L}_{total}$ 
16 return Train encoder  $\mathcal{F}_{\theta^*}$ ;
```

5. Experiments

In this section, we carry out experiments on three publicly available datasets: PlantVillage [16], PlantDoc [43], and Citrus [44], for the plant disease classification task, which serves both to demonstrate the efficacy of the proposed ConMamba model and validate the claims mentioned in the previous sections. Numerical and visual results are carried out successively to evaluate the performance of the proposed model and the quality of the learned features, with comparisons to state-of-the-art methods across various evaluation metrics. Ablation studies were also conducted to evaluate the contribution of encoders and each loss component in enhancing the discrimination between classes across the datasets.

5.1. Datasets

Three datasets, namely PlantVillage, PlantDoc, and Citrus, are used in the experiments, and each of them offers unique features and challenges that provide a proper foundation for assessing the model’s performance across a variety of plant species, diseases, and environmental conditions. A detailed overview of each dataset is presented in the following subsections.

PlantVillage. The PlantVillage [16] is one of the most extensively utilized and publicly accessible resources for PDD research. Developed by Penn State University, it consists of approximately 54,306 high-quality images spanning 14 plant species. It is categorized into 38 classes, including 26 disease classes and 12 healthy classes. The disease categories include 4 bacterial diseases, 17 fungal diseases, 2 viral diseases, 1 mite-induced disease, and 2 mould-related diseases, offering a rich resource for understanding diverse plant health challenges.

PlantDoc. The PlantDoc [43] dataset consists of 2,598 RGB images depicting leaf diseases across 13 plant species. These images are categorized into 28 distinct disease types and are taken directly from natural environments, incorporating real-world conditions such as varying lighting, complex backgrounds, and diverse leaf orientations. This natural diversity enhances the dataset’s complexity, enabling models to learn robust features for real-world disease detection.

Citrus. The Citrus [44] dataset was developed to support research in PDD and classification. It comprises 759 high-resolution images of healthy and diseased citrus fruits and leaves, specifically targeting five major diseases: Black Spot, Canker, Scab, Greening, and

Melanose. For citrus fruits, the dataset includes 150 images categorized into Black Spot, Canker, Greening, Scab, and Healthy. Citrus leaves contain 609 images, classified into Black Spot, Canker, Greening, Melanose, and Healthy. All images were collected from Sargodha, Pakistan, a tropical agricultural region. Our research specifically focuses on the citrus leaf images from this dataset.

5.2. Evaluation Metrics

Four metrics, accuracy [23], precision [45], recall [46], and F1-score [47], are used to evaluate the performance of the proposed method and that of the benchmarks. These metrics provide a comprehensive evaluation of the model’s predictive capabilities, highlighting different aspects of its performance, such as overall correctness, the ability to avoid false positives, and the ability to capture true positives.

5.3. Results and Analysis

5.3.1. Quantitative Performance

The overall performance of the proposed ConMamba framework across the three datasets is summarized in Table 1. ConMamba achieves its highest performance on the PlantVillage dataset, followed by PlantDoc and Citrus. This performance trend reflects the varying levels of dataset complexity. The PlantVillage dataset is relatively simple, as it was collected under controlled conditions, featuring a plain background and a single, centrally positioned leaf in each image. In contrast, the PlantDoc dataset presents greater challenges, as it was captured in natural environments, where images may contain multiple leaves with varying orientations and off-centre placements. The Citrus dataset is the most challenging, as it includes diseased leaves, with some diseases exhibiting similar visual symptoms, making classification more difficult. Despite these challenges, the proposed method consistently achieves over 90% accuracy across all evaluation metrics, demonstrating its robustness and strong potential for accurate PDD.

Table 1: Performance of ConMamba on the three datasets. Evaluation metrics include Accuracy (%), Recall (%), Precision (%), and F1-score (%).

Dataset	Accuracy	Recall	Precision	F1-score
PlantVillage	98.62	97.59	96.74	97.38
PlantDoc	94.29	93.87	93.88	93.97
Citrus	91.38	90.51	91.74	91.66

Table 2: Performance comparison of ConMamba with other self-supervised learning approaches on the **PlantVillage** dataset. Accuracy (%) is used as the evaluation metric, and the top-performing result is highlighted in bold.

Method	Accuracy
Clustering (2022) [23]	88.90
CIKICS (2021) [33]	89.10
CLA (2023) [17]	90.52
CAE and CNN (2021) [48]	98.38
ConMamba (Ours)	98.62

To validate the effectiveness of the proposed ConMamba framework, we conducted comprehensive comparisons with state-of-the-art(SOTA) self-supervised methods, including CAE and CNN (2021) [48], CLA (2023) [17], CNN (2024) [51], MobileNetV3 (2023) [50], Clustering (2022) [23], and BYOL (2020) [35]. These comparisons highlight the robustness and generalizability of our method across three datasets, ranging from controlled to real-world agricultural environments. The results presented in Tables 2-4 demonstrate that the proposed ConMamba achieved significant improvements compared to the existing methods for all three datasets.

Table 2 presents results on the PlantVillage dataset. ConMamba achieves the highest accuracy of 98.62%, outperforming all compared methods. Notably, it surpasses the next best model, CAE and CNN (2021) [48], by 0.24%, and significantly outperforms other approaches such as Clustering (2022) [23], CIKICS (2021) [33], and CLA (2023) [17]. The relatively small improvement margin on this dataset is expected due to its controlled acquisition conditions and minimal background noise.

Table 3: Performance comparison of ConMamba with existing approaches on the **PlantDoc** dataset. Accuracy (%) is used as the evaluation metric, and the top-performing result is highlighted in bold.

Method	Accuracy
InceptionResNetV2 (2020) [43]	70.53
NASNetMobile (2022) [49]	76.48
PI-CNN (2023) [50]	80.36
MobileNetV3 (2023) [50]	83.00
CNN (2024) [51]	87.42
ConMamba (Ours)	94.29

Table 4: Performance comparison of ConMamba with other self-supervised learning approaches on the **Citrus** dataset. Accuracy (%) is used as the evaluation metric, and the top-performing result is highlighted in bold.

Method	Accuracy
CIKICS (2021) [33]	64.10
SimSiam (2021) [36]	87.50
BYOL (2020) [35]	88.90
Clustering (2022) [23]	89.30
ConMamba (Ours)	91.38

In the more complex PlantDoc dataset (Table 3), which contains images captured under natural environmental conditional, ConMamba shows a substantial gain. It achieves 94.29% accuracy, outperforming the second-best method, CNN (2024) [51] by 7.87%. This large improvement reflects ConMamba’s enhanced capability to handle diverse backgrounds, leaf orientations, and lighting variations that often hinder CNN and transformer-based methods.

Table 4 reports performance on the Citrus dataset, which presents a higher degree of class imbalance and visual similarity among disease categories, posing additional challenges for robust disease classification. ConMamba achieves an accuracy of 91.38%, outperforming the next best method Clustering (2022) [23] by 2.08%. This further validates the model’s effectiveness in learning fine-grained distinctions and generalizing well under real-world variability and disease ambiguity.

These consistent improvements across all datasets are attributed to ConMamba’s rich feature representation capabilities, which effectively capture both fine-grained local features and global long-range dependencies. Besides, its dual-level contrastive learning mechanism aligns features at both local(intra-class) and global(inter-class) levels. Moreover, dynamic uncertainty-based loss balancing allows adaptive learning focus, enhancing feature discriminability. In contrast, existing approaches often rely on static loss designs and traditional convolutional backbones, which lack the capacity to model hierarchical spatial relationships and adapt dynamically during training. ConMamba overcomes these limitations, offering a unified and robust framework for self-supervised plant disease detection.

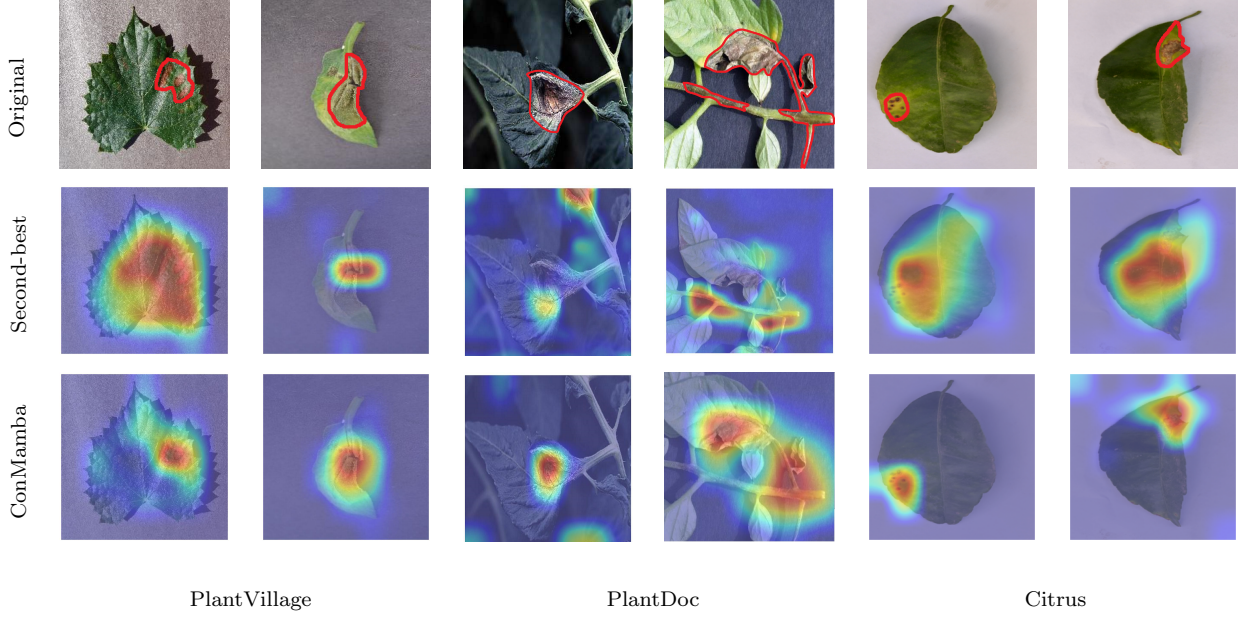


Figure 7: Visualization of activation maps for randomly chosen images from the PlantVillage, PlantDoc, and Citrus datasets. The first row displays the original samples, followed by the second-best method for each dataset (CAE & CNN [48] in PlantVillage, CNN [51] in PlantDoc, and Clustering [23] in Citrus) and the outcomes produced by our proposed ConMamba approach.

5.3.2. Qualitative Performance

To qualitatively assess the discriminative capacity of ConMamba, we generate Class Activation Maps(CAMs) [52] based on the model’s predictions during the testing stage. These visualizations highlight the regions most influential in the model’s decision-making, and show how well it localizes disease symptoms. This visualization provides qualitative evidence of the model’s ability to accurately localize disease-affected areas and differentiate between healthy and diseased regions. Figure 7 presents a side-by-side comparison between ConMamba and the second-best performing methods across three datasets. For each dataset, two representative images are randomly selected. As shown in the figure, ConMamba consistently attends to the most relevant symptomatic regions, while baseline model often exhibit over-extended attention regions or focus on irrelevant areas, leading to misinterpretation and reduced localization precision. These results confirm that ConMamba’s long-range feature modeling and dual-level contrastive learning contribute to more targeted and context-aware spatial attention, which is critical for reliable and fine-grained plant disease classification.

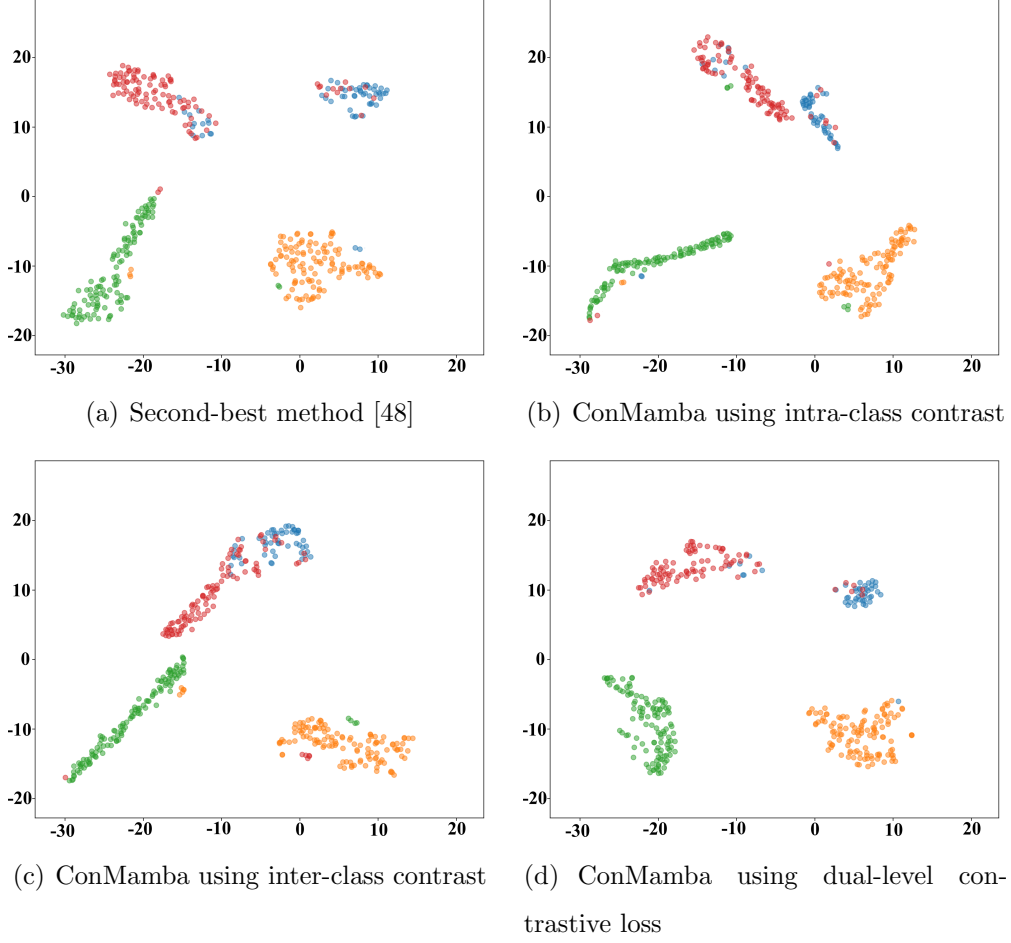


Figure 8: t-SNE visualization of feature representations learned by ConMamba on **corn plant** images from the **PlantVillage dataset**. The plots show the embeddings: (a) second-best method [48], (b) ConMamba using intra-class contrast, (c) ConMamba using inter-class contrast, and (d) ConMamba using dual-level contrastive loss. The figure uses different colors to represent four distinct classes of corn plants. The X and Y axes correspond to the t-SNE Components representing transformed dimensions from the high-dimensional data.

5.4. Ablation Studies

5.4.1. Loss Functions

In this ablation study, we perform a discriminative class analysis using t-SNE [53] to evaluate the effectiveness of the proposed ConMamba model in the test datasets. t-SNE is a non-linear dimensionality reduction technique that visualizes high-dimensional data in two dimensions while preserving local similarities, helping to reveal classification patterns and clusters.

Since the PlantVillage and PlantDoc datasets contain numerous classes (38 and 28, respectively), we selected only the corn plant classes from each dataset to achieve clearer visualisations using t-SNE. Figures 8–10 illustrate the discriminative capabilities of the

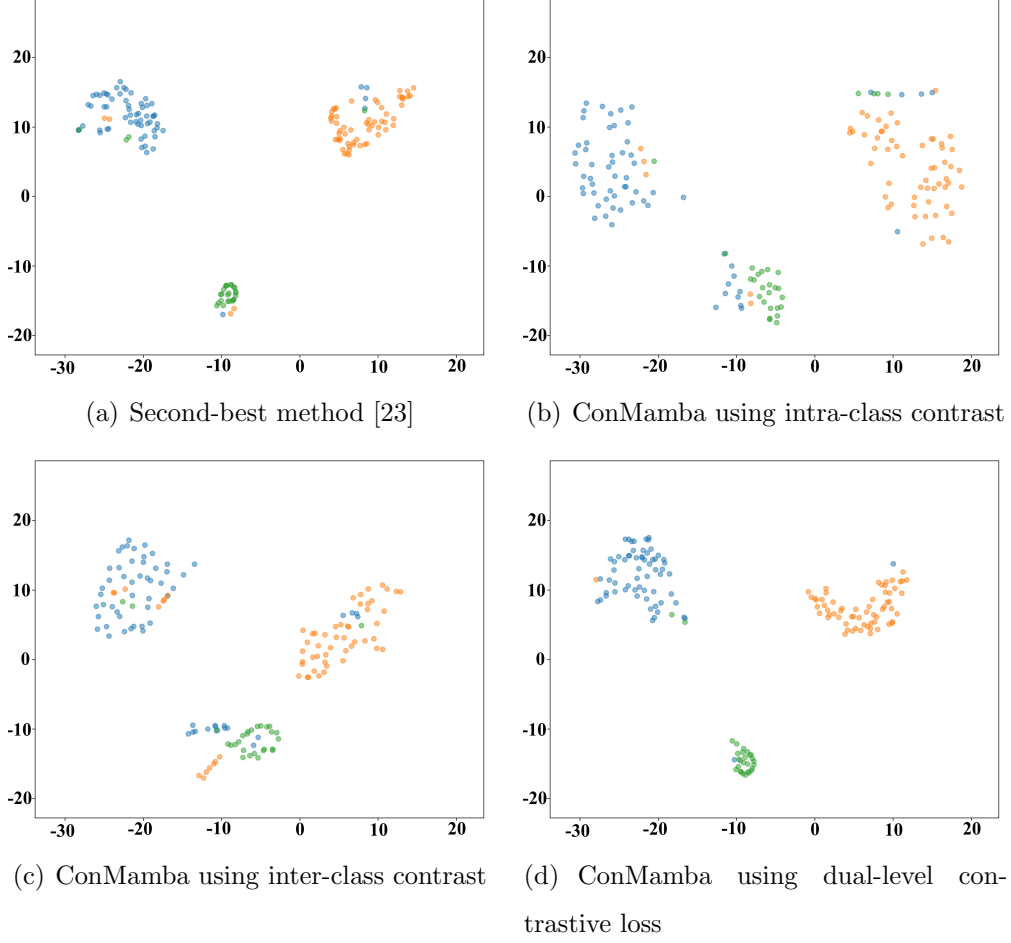


Figure 9: t-SNE visualization of feature representations learned by ConMamba on **corn plant** images from the **PlantDoc** dataset. The plots show the embeddings: (a) second-best method [23], (b) ConMamba using intra-class contrast, (c) ConMamba using inter-class contrast, and (d) ConMamba using dual-level contrastive loss. The figure uses different colors to represent three distinct classes. The X and Y axes correspond to the t-SNE Components representing transformed dimensions from the high-dimensional data.

ConMamba model employing individual loss functions (intra-class contrast and inter-class contrast) compared to the proposed dual-level contrastive loss, alongside the second-best performing models for each dataset.

In Figure 8 (PlantVillage dataset), our proposed dual-level contrastive loss (d) demonstrates the best feature separation, forming well-defined clusters that indicate superior feature learning. Compared to intra-class contrast (b) and inter-class contrast (c), the dual-level contrastive loss produces more clearer cluster boundaries with minimal overlap. In contrast, the second-best method [48] (a) exhibits noticeable cluster overlap, indicating weaker feature extraction. Moving to Figure 9 (PlantDoc dataset), the overall separability of clusters is less distinct than in the PlantVillage dataset, suggesting

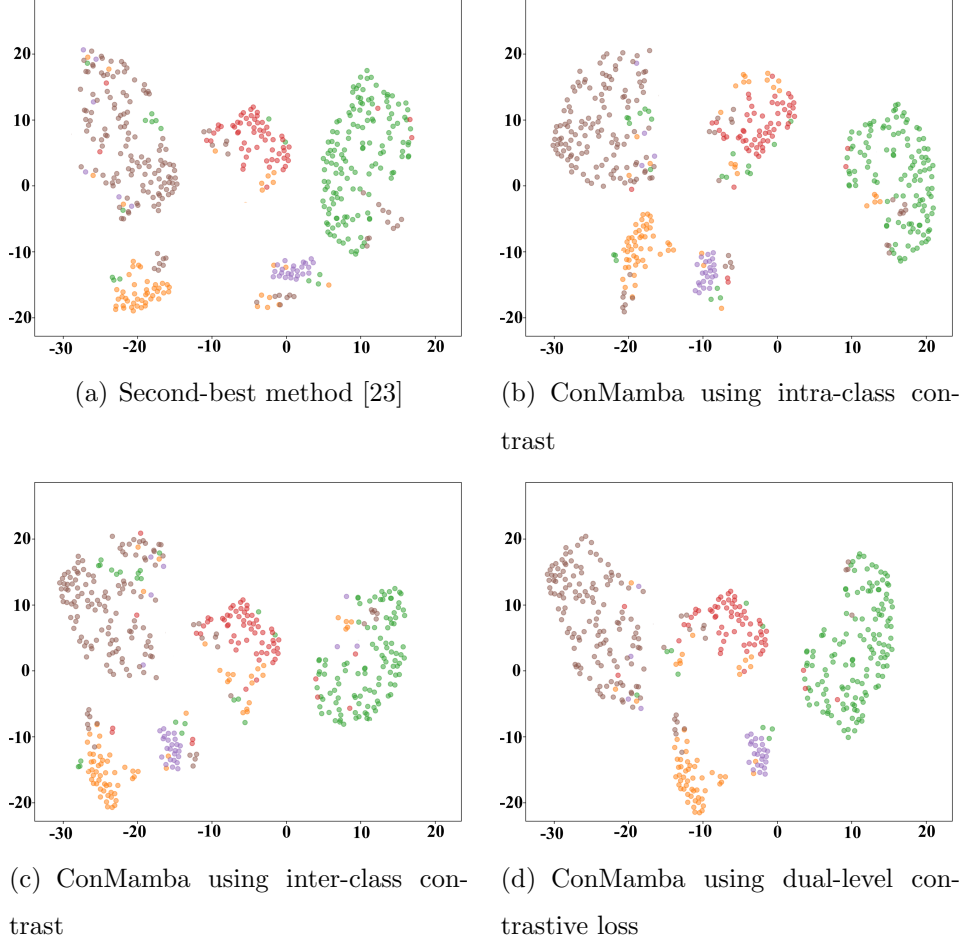


Figure 10: t-SNE visualization of feature representations learned by ConMamba on the **Citrus** dataset. The plots show the embeddings: (a) the second-best method [23], (b) ConMamba using intra-class contrast, (c) ConMamba using inter-class contrast, and (d) ConMamba using dual-level contrastive loss. The figure uses different colors to represent five distinct classes. The X and Y axes correspond to the t-SNE Components representing transformed dimensions from the high-dimensional data.

that PlantDoc is a more challenging dataset. However, our dual-level contrastive loss (d) still outperforms the individual losses and second-best method [23] (a), maintaining clear separation and reducing misclassified points. Finally, in Figure 10 (Citrus dataset), the dual-level contrastive loss (d) again provides the best cluster separation, with clear distinctions between the classes. While the individual losses and second-best method [23] (a) exhibit significant cluster overlaps, reinforcing the effectiveness of the dual-level contrastive learning approach. The improvement trend across all datasets consistently highlights that ConMamba, with the proposed dual-level contrastive loss, substantially improves class discrimination, resulting in superior separation among various plant disease categories relative to alternative approaches.

Table 5: Performance comparison of Vision Mamba and traditional encoder using dual-level contrastive loss on the **PlantVillage** dataset. Evaluation metrics include Accuracy (%), Recall (%), Precision (%), and F1-score (%).

Method	Accuracy	Recall	Precision	F1-score
AlexNet	81.55	81.89	81.33	80.4
MobileNetV3Large	80.75	76.03	76.67	81.34
EfficientNetB0	91.66	88.15	90.31	90.68
VGG16	83.55	81.89	82.33	83.04
ResNet50	93.35	92.5	91.23	90.65
ViT	94.95	94.67	95.55	95.87
VM	98.62	97.59	96.74	97.38

Note: ViT = Vision Transformer; VM = Vision Mamba.

5.4.2. Encoders with Dual-level Contrastive Learning

This ablation study presented in Tables 5–7 illustrates the effectiveness of the proposed VME with dual-level contrastive loss compared to traditional encoders, such as EfficientNetB0, VGG16, ResNet50, and ViT, across the evaluated datasets. VME consistently achieved superior performance, demonstrating accuracy rates of 98.62%, 94.29%, and 91.38%, along with corresponding F1-scores of 97.38%, 93.97%, and 91.66% on the PlantVillage (Table 5), PlantDoc (Table 6), and Citrus (Table 7) datasets, respectively. Comparatively, traditional neural network models such as AlexNet, MobileNetV3Large, EfficientNetB0, VGG16, and ResNet50 exhibited lower performance across all metrics. Among these traditional architectures, ResNet50 and EfficientNetB0 performed better than AlexNet and MobileNetV3Large, though still significantly behind VM. In particular, ViT showed competitive results, particularly in the PlantVillage dataset, achieving an accuracy of 94.95% and an F1 score of 95.87%, but remained consistently below VM in all metrics and test datasets. These observations emphasize the robustness and effectiveness of the proposed VME with dual-level contrastive learning as a superior approach for plant disease classification.

Table 6: Performance comparison of Vision Mamba and traditional encoder using dual-level contrastive loss on the **PlantDoc** dataset. Evaluation metrics include Accuracy (%), Recall (%), Precision (%), and F1-score (%).

Method	Accuracy	Recall	Precision	F1-score
AlexNet	85.27	81.75	81.82	82.24
MobileNetV3Large	87.75	86.03	86.67	86.34
EfficientNetB0	88.69	87.47	85.62	86.97
VGG16	87.55	86.89	87.33	87.04
ResNet50	89.8	88.67	88.06	89.18
ViT	91.78	90.54	91.63	91.52
VM	94.29	93.87	93.88	93.97

Note: ViT = Vision Transformer; VM = Vision Mamba.

Table 7: Performance comparison of Vision Mamba and traditional encoder using dual-level contrastive loss on the **Citrus** dataset. Evaluation metrics include Accuracy (%), Recall (%), Precision (%), and F1-score (%).

Method	Accuracy	Recall	Precision	F1-score
AlexNet	82.31	81.88	81.75	81.28
MobileNetV3Large	80.85	76.13	76.57	81.44
EfficientNetB0	83.16	82.13	81.46	81.74
VGG16	82.45	81.79	82.23	83.14
ResNet50	83.56	82.92	81.4	80.63
ViT	89.63	88.54	87.23	88.73
VM	91.38	90.51	91.74	91.66

Note: ViT = Vision Transformer; VM = Vision Mamba.

6. Conclusion

In this paper, we propose ConMamba, a novel self-supervised learning framework designed for plant disease detection (PDD), aiming to reduce dependence on large, annotated datasets. By leveraging unlabelled data, ConMamba learns rich and discriminative feature representations that improve classification performance across diverse and challenging scenarios. Specifically, ConMamba is based on the state-space model, which efficiently captures long-range dependent features. Long-range dependence is particularly

important for PDD because disease symptoms can appear as subtle, scattered patterns across a leaf. By enhancing these long-range correlations, the model can integrate information from various regions of the leaves/plants. Thereby capturing the overall context and structure of the affected areas. Besides, we propose a dual-level contrastive learning strategy with a dynamic uncertainty-based loss weighting mechanism that aligns local and global features, enabling the model to effectively learn both fine-grained details and global structure. Extensive experiments on three benchmark datasets and comprehensive ablation studies validate the effectiveness and robustness of ConMamba. Future work will focus on refining the dynamic integration strategies, expanding the framework to additional datasets, and exploring its broader applications in precision agriculture and sustainable farming practices.

References

- [1] R. N. Jogekar, N. Tiwari, A review of deep learning techniques for identification and diagnosis of plant leaf disease, *Smart Trends in Computing and Communications: Proceedings of SmartCom 2020* (2021) 435–441.
- [2] S. Gupta, S. Verma, R. Thakur, Phytosanitary requirement for import of horticulture crops, *Int. J. Curr. Microbiol. App. Sci* 8 (2) (2019) 2871–2886.
- [3] R. Dwivedi, S. Dey, C. Chakraborty, S. Tiwari, Grape disease detection network based on multi-task learning and attention features, *IEEE Sensors Journal* 21 (16) (2021) 17573–17580.
- [4] L. C. Ngugi, M. Abelwahab, M. Abo-Zahhad, Recent advances in image processing techniques for automated leaf pest and disease recognition—a review, *Information processing in agriculture* 8 (1) (2021) 27–51.
- [5] Y. Hu, J. Zhan, G. Zhou, A. Chen, W. Cai, K. Guo, Y. Hu, L. Li, Fast forest fire smoke detection using mvmmnet, *Knowledge-Based Systems* 241 (2022) 108219.
- [6] D. Ahmedt-Aristizabal, D. Smith, M. R. Khokher, X. Li, A. L. Smith, L. Petersson, V. Roland, E. J. Edwards, An in-field dynamic vision-based analysis for vineyard yield estimation, *IEEE Access* (2024).
- [7] M. I. Hossen, M. Awrangjeb, S. Pan, A. A. Mamun, Transfer learning in agriculture: a review, *Artificial Intelligence Review* 58 (4) (2025) 97.

- [8] S. Ashwinkumar, S. Rajagopal, V. Manimaran, B. Jegajothi, Automated plant leaf disease detection and classification using optimal mobilenet based convolutional neural networks, *Materials Today: Proceedings* 51 (2022) 480–487.
- [9] P. Bansal, R. Kumar, S. Kumar, Disease detection in apple leaves using deep convolutional neural network, *Agriculture* 11 (7) (2021) 617.
- [10] J. Yang, X. Guo, Y. Li, F. Marinello, S. Ercisli, Z. Zhang, A survey of few-shot learning in smart agriculture: developments, applications, and challenges, *Plant Methods* 18 (1) (2022) 28.
- [11] R. G ldenring, L. Nalpantidis, Self-supervised contrastive learning on agricultural images, *Computers and Electronics in Agriculture* 191 (2021) 106510.
- [12] L. Zhang, G. Zhou, C. Lu, A. Chen, Y. Wang, L. Li, W. Cai, Mmdgan: A fusion data augmentation method for tomato-leaf disease identification, *Applied Soft Computing* 123 (2022) 108969.
- [13] Y. Zhao, Z. Chen, X. Gao, W. Song, Q. Xiong, J. Hu, Z. Zhang, Plant disease detection using generated leaves based on doublegan, *IEEE/ACM Transactions on Computational Biology and Bioinformatics* 19 (3) (2021) 1817–1826.
- [14] Y. LeCun, L. Bottou, Y. Bengio, P. Haffner, Gradient-based learning applied to document recognition, *Proceedings of the IEEE* 86 (11) (1998) 2278–2324.
- [15] W. Wang, E. Xie, X. Li, D.-P. Fan, K. Song, D. Liang, T. Lu, P. Luo, L. Shao, Pyramid vision transformer: A versatile backbone for dense prediction without convolutions, in: *Proceedings of the IEEE/CVF international conference on computer vision*, 2021, pp. 568–578.
- [16] A. Al Mamun, D. Ahmedt-Aristizabal, M. Zhang, M. I. Hossen, Z. Hayder, M. Awrangjeb, Plant disease detection using self-supervised learning: A systematic review, *IEEE Access* (2024).
- [17] R. Zhao, Y. Zhu, Y. Li, CLA: a self-supervised contrastive learning method for leaf disease identification with domain adaptation, *Computers and Electronics in Agriculture* 211 (2023) 107967.
- [18] H. Zhang, Y. Cao, Understanding the benefits of simclr pre-training in two-layer convolutional neural networks, *arXiv preprint arXiv:2409.18685* (2024).

- [19] T. Kim, H. Kim, K. Baik, Y. Choi, Instance-aware plant disease detection by utilizing saliency map and self-supervised pre-training, *Agriculture* 12 (8) (2022) 1084.
- [20] H. Jin, X. Chu, J. Qi, X. Zhang, W. Mu, CWAN: Self-supervised learning for deep grape disease image composition, *Engineering Applications of Artificial Intelligence* 123 (2023) 106458.
- [21] T. Chen, S. Kornblith, M. Norouzi, G. Hinton, A simple framework for contrastive learning of visual representations, in: *International conference on machine learning*, PMLR, 2020, pp. 1597–1607.
- [22] H. Hu, X. Wang, Y. Zhang, Q. Chen, Q. Guan, A comprehensive survey on contrastive learning, *Neurocomputing* (2024) 128645.
- [23] M. M. Monowar, M. A. Hamid, F. A. Kateb, A. Q. Ohi, M. Mridha, Self-supervised clustering for leaf disease identification, *Agriculture* 12 (6) (2022) 814.
- [24] S. Bunyang, N. Thedwichienchai, K. Pintong, N. Lael, W. Kunaborimas, P. Boonrat, T. Siriborvornratanakul, Self-supervised learning advanced plant disease image classification with simclr, *Advances in Computational Intelligence* 3 (5) (2023) 18.
- [25] S. Huaquipaco, O. Vera, V. Yana-Mamani, W. Mamani, H. Calsina, F. Puma, E. Morales-Rojas, N. Beltran, J. Cruz, Peacock spot detection in olive leaves using self supervised learning in an assembly meta-architecture, *IEEE Access* (2024).
- [26] J. Zhang, H. Guo, J. Guo, J. Zhang, An information entropy masked vision transformer (iem-vit) model for recognition of tea diseases, *Agronomy* 13 (4) (2023) 1156.
- [27] X. Yu, J. Wang, Y. Zhao, Y. Gao, Mix-vit: Mixing attentive vision transformer for ultra-fine-grained visual categorization, *Pattern Recognition* 135 (2023) 109131.
- [28] X. Zhang, H. Zeng, S. Guo, L. Zhang, Efficient long-range attention network for image super-resolution, in: *European conference on computer vision*, Springer, 2022, pp. 649–667.
- [29] B. Yang, X. Xiang, W. Kong, Y. Peng, J. Yao, Adaptive multi-task learning using lagrange multiplier for automatic art analysis, *Multimedia Tools and Applications* (2022) 1–19.
- [30] A. Gu, T. Dao, Mamba: Linear-time sequence modeling with selective state spaces, *arXiv preprint arXiv:2312.00752* (2023).

- [31] A. Gu, K. Goel, C. Ré, Efficiently modeling long sequences with structured state spaces, arXiv preprint arXiv:2111.00396 (2021).
- [32] L. Li, S. Zhang, B. Wang, Plant disease detection and classification by deep learning—a review, *IEEE Access* 9 (2021) 56683–56698.
- [33] U. Fang, J. Li, X. Lu, L. Gao, M. Ali, Y. Xiang, Self-supervised cross-iterative clustering for unlabeled plant disease images, *Neurocomputing* 456 (2021) 36–48.
- [34] G. Yang, G. Chen, Y. He, Z. Yan, Y. Guo, J. Ding, Self-supervised collaborative multi-network for fine-grained visual categorization of tomato diseases, *IEEE Access* 8 (2020) 211912–211923.
- [35] J.-B. Grill, F. Strub, F. Altché, C. Tallec, P. Richemond, E. Buchatskaya, C. Doersch, B. Avila Pires, Z. Guo, M. Gheshlaghi Azar, et al., Bootstrap your own latent—a new approach to self-supervised learning, *Advances in neural information processing systems* 33 (2020) 21271–21284.
- [36] X. Chen, K. He, Exploring simple siamese representation learning, in: *Proceedings of the IEEE/CVF conference on computer vision and pattern recognition*, 2021, pp. 15750–15758.
- [37] H. Zhang, Y. Xu, J. Sun, Detection of cassava leaf diseases using self-supervised learning, in: *2021 2nd International Conference on Computer Science and Management Technology (ICCSMT)*, IEEE, 2021, pp. 120–123.
- [38] J. Zhang, H. Guo, J. Guo, J. Zhang, An information entropy masked vision transformer (iem-vit) model for recognition of tea diseases, *Agronomy* 13 (4) (2023) 1156.
- [39] X. Yu, J. Wang, Y. Zhao, Y. Gao, Mix-ViT: Mixing attentive vision transformer for ultra-fine-grained visual categorization, *Pattern Recognition* 135 (2023) 109131.
- [40] Y. Meng, M. Xu, H. Kim, S. Yoon, Y. Jeong, D. S. Park, Known and unknown class recognition on plant species and diseases, *Computers and Electronics in Agriculture* 215 (2023) 108408.
- [41] K. He, H. Fan, Y. Wu, S. Xie, R. Girshick, Momentum contrast for unsupervised visual representation learning, in: *Proceedings of the IEEE/CVF conference on computer vision and pattern recognition*, 2020, pp. 9729–9738.
- [42] J. G. A. Barbedo, A review on the main challenges in automatic plant disease identification based on visible range images, *Biosystems engineering* 144 (2016) 52–60.

- [43] D. Singh, N. Jain, P. Jain, P. Kayal, S. Kumawat, N. Batra, PlantDoc: A dataset for visual plant disease detection, in: Proceedings of the 7th ACM IKDD CoDS and 25th COMAD, 2020, pp. 249–253.
- [44] H. T. Rauf, B. A. Saleem, M. I. U. Lali, M. A. Khan, M. Sharif, S. A. C. Bukhari, A citrus fruits and leaves dataset for detection and classification of citrus diseases through machine learning, *Data in brief* 26 (2019) 104340.
- [45] Y. Wang, Y. Yin, Y. Li, T. Qu, Z. Guo, M. Peng, S. Jia, Q. Wang, W. Zhang, F. Li, Classification of plant leaf disease recognition based on self-supervised learning, *Agronomy* 14 (3) (2024) 500.
- [46] Y. Cao, G. Sun, Y. Yuan, L. Chen, Small-sample cucumber disease identification based on multimodal self-supervised learning, *Crop Protection* 188 (2025) 107006.
- [47] A. Al Mamun, P. P. Em, M. J. Hossen, B. Jahan, A. Tahabilder, A deep learning approach for lane marking detection applying encode-decode instant segmentation network, *Heliyon* 9 (3) (2023).
- [48] P. Bedi, P. Gole, Plant disease detection using hybrid model based on convolutional autoencoder and convolutional neural network, *Artificial Intelligence in Agriculture* 5 (2021) 90–101.
- [49] P. Enkvetchakul, O. Surinta, Stacking ensemble of lightweight convolutional neural networks for plant leaf disease recognition, *ICIC Express Letters* 16 (5) (2022) 521–528.
- [50] T.-A. Nguyen, T.-M. Hoang, D.-M. Tran, An effective deep learning model for detecting plant diseases using a natural dataset for the agricultural iot system, in: International Conference on Intelligence of Things, Springer, 2023, pp. 136–147.
- [51] B. Chung, Addressing data imbalance in plant disease recognition through contrastive learning, in: 2024 IEEE 3rd International Conference on AI in Cybersecurity (ICAIC), IEEE, 2024, pp. 1–6.
- [52] X. Yu, Y. Zhao, Y. Gao, S. Xiong, Maskcov: A random mask covariance network for ultra-fine-grained visual categorization, *Pattern Recognition* 119 (2021) 108067.
- [53] L. Van der Maaten, G. Hinton, Visualizing data using t-sne., *Journal of machine learning research* 9 (11) (2008).